Valorisation of energy plant *Arundo donax* cultivated in Serbia for biosorption of cobalt ions from an aqueous solution: kinetic aspect

Jovana Perendija[1], Dragana Milošević[1], Mina Popović[1], Željko Dželetović[2], Sabina Kovač[3], Jasmina Grbović Novaković[4] and Slobodan Cvetković[1]

[1]*University of Belgrade, Institute of Chemistry, Technology, and Metallurgy, National Institute of the Republic of Serbia, Belgrade, Serbia*
[2]*University of Belgrade, INEP Institute for the Application of Nuclear Energy, Zemun-Belgrade, Serbia*
[3]*University of Belgrade, Faculty of Mining and Geology, Belgrade, Serbia*
[4]*University of Belgrade, "Vinča" Institute of Nuclear Sciences, National Institute of Serbia, Centre of Excellence for Hydrogen and Renewable Energy, Belgrade, Serbia*

Abstract
Metal ions can be eliminated from aqueous solutions using biosorbent, a substance made from plant biomass. This study investigated the potential use of *Arundo donax* stems as a cheap, natural biosorbent to remove cobalt ions (Co^{2+}) from an aqueous solution. The biosorbent was characterized by the chemical composition analysis (cellulose, hemicellulose, and lignin), the point of zero charge (pH_{PZC}), by scanning electron microscopy, energy dispersive spectroscopy, X-ray diffraction analysis, and Fourier-transform infrared spectroscopy. According to the experimental data of kinetic studies, the equilibrium condition of Co^{2+} adsorption was attained 360 min after the biosorption started. The pseudo-first, pseudo-second, Elovich, and intra-particle diffusion models were used to model the kinetic experimental data. The best compliance was obtained with the pseudo-first order kinetic model, considering the highest value of the coefficient of determination R^2 (0.996) and the lowest chi-square (χ^2) value (0.757). The findings of this study can be applied to the design of batch biosorption systems for the removal of Co^{2+} ions in real industrial systems.

Keywords: Biosorbent; Co^{2+} removal; kinetic modeling.

Available on-line at the Journal web address: http://www.ache.org.rs/HI/

ORIGINAL SCIENTIFIC PAPER

UDC: 661.183.122:546.732:532.73

Hem. Ind. **78(3)** 253-264 (2024)

1. INTRODUCTION

The human population is faced with problems related to water pollution. Industrial systems generated large amounts of wastewater and after processing, the contaminated water is discharged into a recipient, posing risks to aquatic life as it contains many polluting substances. Among them, the presence of various harmful heavy metals (e.g. iron, lead, nickel, silver, lead, cadmium, copper, manganese, etc.) is one of the largest environmental issues due to moderate accumulation over time in organisms.

Cobalt can be found in the natural environment along with iron, nickel, silver, lead, copper, manganese, and other elements [1]. It is also present in igneous and sedimentary rocks. It can also be often found in nuclear power plant wastewater and wastewater from numerous other industries, including mining, metallurgical, electroplating, paints, pigments, and electronic industries. The ecosystem is negatively impacted by cobalt as a harmful element. Numerous health issues, including paralysis, diarrhea, lung irritation, and bone abnormalities, may be induced by high cobalt levels [2]. Heavy metals could be removed from wastewater by using a variety of processes, including adsorption, sedimentation and flocculation, coprecipitation, complexation, heavy metal uptake by wetlands, photo-catalysis, solvent extraction, ion exchange, chemical precipitation, membrane separation techniques, oxidation/reduction, and electro-remediation [3,4]. The use of bio-waste-derived adsorbents is recommended because of their superior efficiency, low cost, and minimal environmental problems. One such cutting-edge technique is biosorption, which is

Corresponding authors:Slobodan Cvetković, Institute of Chemistry, Technology and Metallurgy, National Institute of the Republic of Serbia, Njegoševa 12, 11000 Belgrade, Serbia
Paper received: 17 July 2023; Paper accepted: 21 August 2024; Paper published: 19 September 2024.
E-mail: slobodan.cvetkovic@ihtm.bg.ac.rs
https://doi.org/10.2298/HEMIND240713017P

based on development of biosorbents from a variety of readily available plant materials, including husks, leaves, peels, stems, branches, and pods. There are significant efforts being made in this area to prepare innovative, low-cost bio-waste-based adsorbents that are effective at removing heavy metals from wastewater [5].

Arundo donax (common name: Giant reed) is planted in many regions such as tropical Asia and the Mediterranean and cultivation of this plant has a potential considering that it is a fast-growing invasive plant [6]. In Europe, this area covers inland along the major rivers of the Iberian Peninsula and along the Mediterranean coast from Spain to Greece, including the Adriatic coast. The plant may thrive on salty and arid soils [6]. *Arundo donax* is a very suitable source of biomass because of its low cost and high production. It also contains large amounts of cellulose and lignin, which has led to its widespread use globally for a range of applications such as production of energy, paper pulp, and wooden building materials, among others. Research indicates that *A. donax* L. can withstand challenging environmental conditions, such as the presence of toxic heavy metals [7]. Its ability to accumulate heavy metals in the tissues [8] led to the use of this plant directly as a biosorbent [9,10].

This work aimed to estimate removal of Co^{2+} ions from aqueous phase by unmodified powdered stems of *A. Donax* in batch biosorption experiments. After detailed characterization of pulverized stems of *Arundo donax*, biosorption kinetics was studied. Further, the experimental results were modeled using four different kinetic models (pseudo-first, pseudo-second, Elovich, and intra-particle diffusion model). The aim also was to examine the possibility of modelling of cost-effective and environmentally friendly process for the removal of Co^{2+} from the contaminated water system.

2. MATERIAL AND METHODS

2. 1. Chemicals and materials

Sodium hydroxide, hydrochloric acid (37 %), and AAS cobalt (Co^{2+}) standard solution (1000 mg dm^{-3}) were supplied from Merck, Germany. Dilute solutions (0.1 M NaOH and 0.1 M HCl) were used for pH adjustment and synthetic Co^{2+} stock solution was prepared with ultrapure water (Milli-Q system by Merck). The waste *Arundo donax* stems used in this study were provided by the Institute for the Application of Nuclear Energy - INEP, Belgrade, Serbia. The leached chernozem as soil type was used to cultivate *Arundo donax*.

2. 2. Preparation methods

Biosorbent from waste *Arundo donax* stems was prepared as follows: the sample was washed with deionized water several times in order to remove the impurities, and then was chopped. Next, it was dried in an oven at 70 °C for 12 h, and the dried stems were chopped in a blender. The fraction with a particle size smaller than 0.5 mm was used in the experiments. The prepared biosorbent is labelled as W-ADs and was stored in plastic containers in a desiccator until use.

2. 3. Characterization of W-ADs biosorbent

1. 3. 1. Lignocellulose composition

The lignocellulose composition (cellulose, hemicellulose, and lignin) of the W-Ads biosorbent was determined in compliance with standards ISO16472:2006 and ISO13906:2008 [11,12].

2. 3. 2. Structural and morphological characterization

Fourier-transform infrared spectroscopy in attenuated total reflectance mode (ATR-FTIR) of a sample W-Ads was performed by using a Thermo Scientific Nicolet 6700 spectrometer (Thermo Fisher Scientific, USA) in the range of wavenumbers 4000 - 500 cm^{-1}. The sample morphology was analyzed by field emission scanning electron microscopy (FE-SEM), by using the instrument SEM FEI Scios2 Dual Beam System (Thermo Fisher Scientific, USA), after providing conductivity by sputtering the sample with a thin golden layer. The energy dispersive spectroscopy (EDS) analysis was performed by using an EDS detector integrated with the SEM FEI Scios2 Dual Beam System (Thermo Fisher Scientific, USA). X-ray diffraction analysis (XRD) was used to determine the phase composition of the sample using Rigaku SmartLab powder X-ray diffractometer (Rigaku, Japan) with Cu-Kα radiation, at room temperature.

2. 3. 3. Determination of the point of zero charge

For determination of the point of zero charge (pH_{PZC}), 100 mg of the biosorbent samples were shaken in 50 cm^3 of NaCl solution (0.01 M) for 24 h at 25 °C and at six different pH values (2, 4, 6, 8, 10, and 12). Afterward, the biosorbent samples were separated from the solution by decantation. The solution pH values were measured by a WTW inoLab 730 pH meter (WTW, Germany,). The pH_{PZC} value of the W-ADs biosorbent was obtained from the plot of the initial vs. final pH value (pH_{final} *vs.* $pH_{initial}$). The intersection point of the curve obtained from this plot and the diagonal gave the pH_{PZC} value [13].

2. 4. Distribution of Co^{2+} ionic species

A speciation diagram of Co^{2+} ions in an aqueous solution as a function of pH was drawn using the Visual MINTEQ software (version 3.1, Department of Land and Water Resources Engineering, Stockholm, Sweden).

2. 5. Biosorption experiments

A kinetic study in a batch system was performed with the goal to evaluate the performance of the W-ADs biosorbent. The experiment was conducted by mixing the known biosorbent dosage (2 g dm^{-3}) in 100 cm^3 Erlenmeyer flasks containing 50 cm^3 of a 100 mg $dm^{-3}$of Co^{2+} solution at 25 °C and pH 7. Samples (50 cm^3) were taken at equal time intervals. All experiments were conducted in triplicate. The Co^{2+} solutions were filtrated by a nylon syringe filter (0.22 μm). The concentration of remaining Co^{2+} ions in the solution was determined by using an AA spectrometer (PinAAcle 900T-PerkinElmer, Massachusetts, USA).

The biosorption capacity (q_e / mg g^{-1}), and removal efficiency of Co^{2+} (R_e / %), were calculated according to Equations (1) and (2):

$$q_e = (C_0 - C_e)V/m \quad (1)$$

$$R_e = 100(C_0\text{-}C_e)/C_0 \quad (2)$$

where C_0 and C_e are Co^{2+} concentrations before and after biosorption, respectively, V is the volume of solution, and m is the mass of the W-ADs biosorbent.

The kinetics of the Co^{2+} biosorption on the W-ADs was analysed, using the pseudo-first order, pseudo-second order, Elovich, and intra-particle diffusion models [14] applied to the experimental data.

2. 5. 1. Pseudo-first order model

The pseudo-first order rate can be expressed by Equation (3):

$$\ln(q_e\text{-}q_t) = \ln q_e\text{-}k_1 t \quad (3)$$

where, q_e is the equilibrium biosorption capacity (contentof Co^{2+} per mass of the biosorbent), q_t is the biosorbed content of Co^{2+} per mass of the biosorbent at the time t, and k_1 is the pseudo-first order rate constant.

2. 5. 2. Pseudo-second order model

The pseudo-second order model can be expressed by Equation (4):

$$t/q_t = \left(k_2 q_e^{\,2}\right)^{-1} + t/q_e \quad (4)$$

where k_2 is the equilibrium constant of the pseudo-second order reaction rate.

2. 5. 3. Elovich model

The simplified equation of the Elovich model is described as follows, Equation (5):

$$q_t = 1/b\,ln(ab) + 1/b\,\ln t \quad (5)$$

where a / mg g^{-1} min^{-1} is the initial biosorption rate constant, and b / g mg^{-1} is the desorption rate constant of the Elovich model.

2. 5. 4. Intra-particle diffusion model

Possibility that the biosorption rate is controlled by intra-particle diffusion was tested by using the following simplified Equation (6):

$$q_t = k_{dif} t^{1/2} \quad (6)$$

where k_{dif} is the intra-particle diffusion rate constant. For diffusion through a spherical particle, this model should be applicable if the plot passes through the origin and follows a linear trend when the following condition is met $q_t/q_e < 0.4$ (*i.e.* in the early adsorption times until 40 % of the equilibrium amount is adsorbed) [15].

3. RESULTS AND DISCUSSION

3. 1. Lignocellulose composition of W-ADs biosorbent

Contents of cellulose, hemicellulose, and lignin for the W-Ads sample are represented in Table 1.

Table 1. Lignocellulose composition analysis of the W-ADs biosorbent

Component	Content, wt.%, (dry basis)
Cellulose	36.60
Hemicellulose	25.44
Lignin	35.24

A review of the literature revealed that the contents of cellulose, hemicellulose, and lignin in *Arundo donax* vary. Close values of cellulose (35.52 and 35.6 %) and hemicellulose contents (26.81 and 24 %) as in the present study (Table 1) are found in the literature [16,17]. Lignin content for raw milled material is much higher than that for processed fibres, accounting for around 35 % [18] similarly as it was obtained in the present study (35.24 %). Some authors have reported similar values for total lignin, approximately 33.65 % [19] and 30 % [20].

Differences in the lignocellulose composition in *Arundo donax* samples are attributed to various factors such as plant maturity, region, soil physiognomies, share of stem components, sample preparation techniques, etc. The comparative analysis of stem composition showed some differences between nodes and internodes. The nodes have similar lignin contents (~21 %) but they are richer in hemicelluloses (32.0 *vs.* 28.5 %) and poorer in cellulose (29.2 *vs.* 32.9%), as compared with internodes [21].

3. 2. Structural characterization by FTIR spectroscopy

The FTIR spectrum of a W-ADs sample is presented in Figure 1. It was used for the analysis of surface functional groups, providing insights into the nature and composition of the biomass. As expected in similar plant cultures made of lignocellulose, the FTIR spectrum of a tested sample, confirmed the presence of hemicellulose, cellulose, and lignin. These three components are considered as three major components of lignocellulosic materials [22].

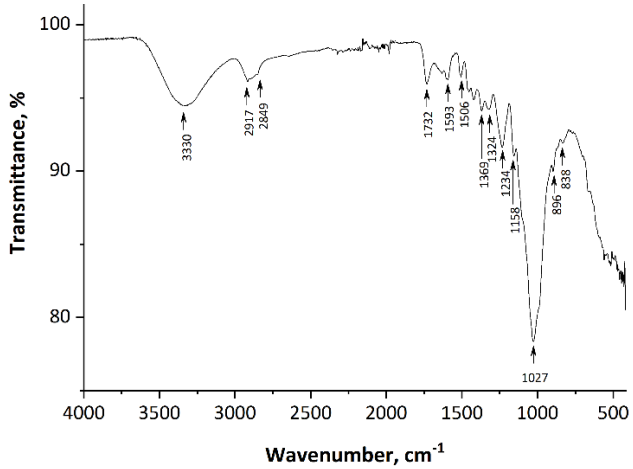

Figure 1. FTIR spectrum of a W-ADs sample

The broad band between 3400-3600 cm^{-1} was attributed to the stretching vibration of the hydrogen-bonded hydroxyl groups originating from cellulose. Bands at 2917 and 2849 cm^{-1} were assigned to C-H stretching vibrations from -CH_2 and -CH_3 components in cellulose and hemicellulose [23]. Besides the absorption band at 1732 cm^{-1} originating from a C=O stretching vibration [23] of acetyl groups in hemicellulose, the band present at 1234 cm^{-1} could also indicate a presence of hemicellulose i.e. its acetyl ester units [24]. Also, according to Galletti *et al.* [25], a small peak at 1732 cm^{-1} may indicate the presence of C=O ester bonds of ferulic and/or p-coumaric acids, which are bonded together with hemicellulose. According to Fiore *et al.* [23], the peak with a maximum cantered at 1506 cm^{-1} could be attributed to C=C stretching vibrations of the benzene ring of the lignin molecule. Bands between 1450 and 1200 cm^{-1} could be assigned to C-H vibrations of the CH_2 and CH_3 groups. In the region between 1200 and 850 cm^{-1} absorption bands typical for cellulose are noticed, as well as, in the region between 1550 and 1300 cm^{-1} corresponding to bands related to lignin [25]. It is known that materials of plant origin among other components contain polysaccharides, and bands indicating the presence of polysaccharides molecules are present in the spectral region 1000-1200 cm^{-1} corresponding to C-O-C, C-C and C-O vibrations [25]. The characteristic C-H and C-O bending vibrations of the aromatic ring in polysaccharides are observed at 1369 and 1324 cm^{-1}, respectively.

3. 3. SEM analysis of W-ADs biosorbent microstructure

The surface morphology of a W-ADs sample obtained by SEM is presented in Figure 2 showing a rough, corrugated surface layer with decreased porosity, clear gaps, and cracks. Furthermore, moderately developed surface of W-ADs can be observed with, certain impurities that are typical for raw natural materials.

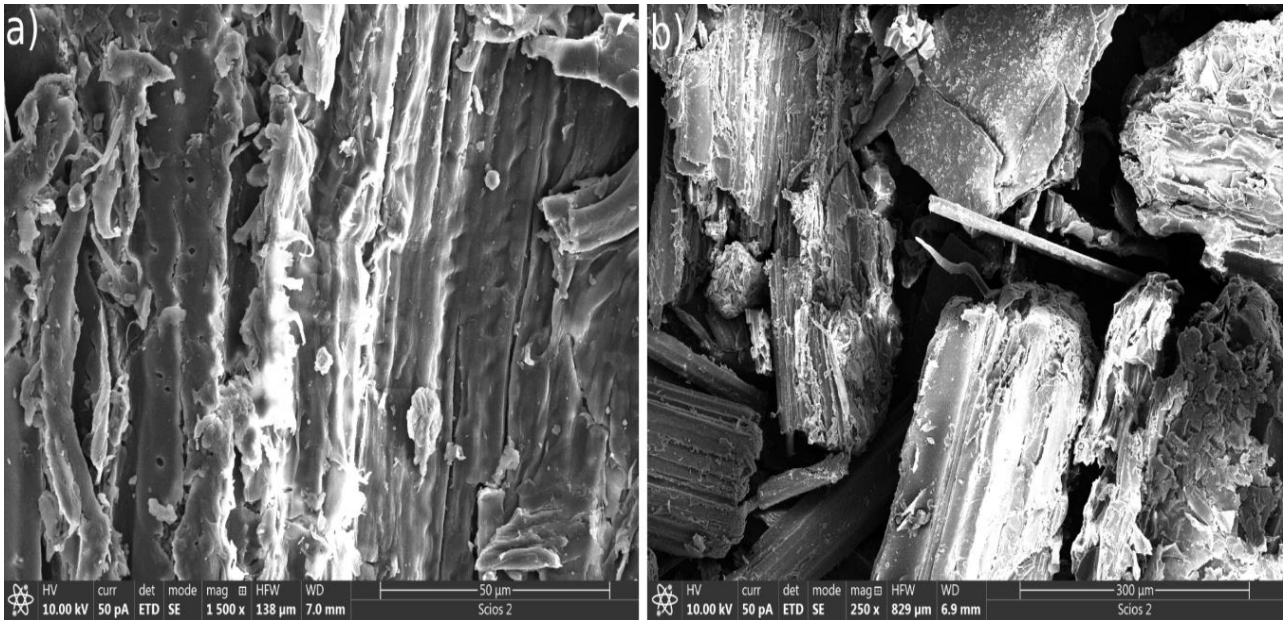

Figure 2. SEM micrographs of a W-ADs sample at different magnifications

3. 4. Energy dispersive spectroscopy analyses

EDS spectra of the biosorbent (Fig. 3) showed the presence of C and O as the major constituents, and Si to a lesser extent. The presence of Si (1.596 wt. %) indicates the existence of bilobate phytoliths in the material [26]. Besides the EDS elemental mapping for O, C and Si (Fig. 3b-d), values of the mass percentage of these elements in the tested area are shown in Figure 3e.

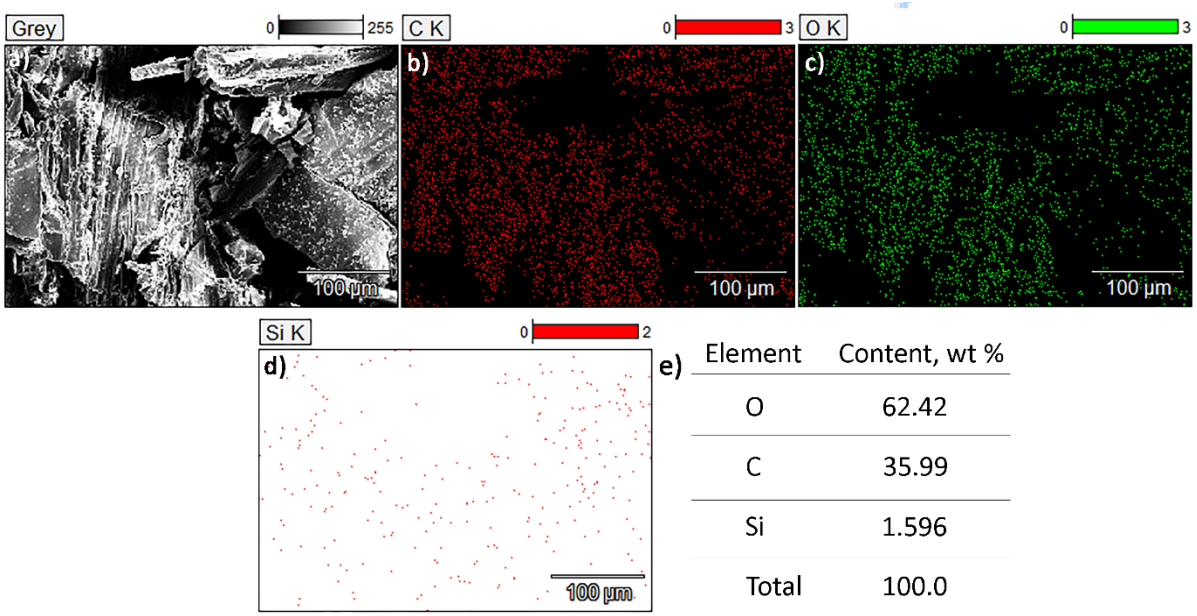

Element	Content, wt %
O	62.42
C	35.99
Si	1.596
Total	100.0

Figure 3. SEM image of W-ADs a) corresponding EDS elemental mapping for O, C and Si (b-d) and element composition e)

3. 5. XRD analysis

X-ray diffraction was applied to determine the presence of amorphous and crystalline phases in the W-ADs biosorbent (Fig. 4). the obtained peak of the strongest intensity between 22 and 23° 2θ with slightly weaker reflections at 2θ ~20.5 and ~34.5°, corresponds to cellulose I. Broad peaks indicate amorphous structure *of Arundo donax*. It is a consequence of the presence of other amorphous components such as hemicellulose, lignin and disordered cellulose, which together contribute to the amorphous phase signal of the W-ADs sample.

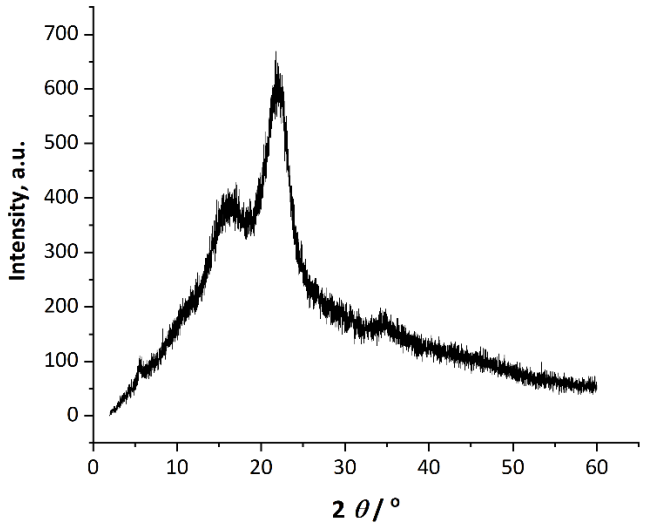

Figure 4. XRD pattern of a W-Ads sample

3. 6. Point of zero charge

Figure 5 shows determination of the point of zero charge (pH_{PZC}) value, which was estimated as 6.89. Generally, it is a well-known fact that a biosorbent surface is positively charged when the solution pH is lower than the pH_{PZC} value, and on the contrary, when pH is higher than the pH_{PZC} value, the biosorbent surface is negatively charged. Considering the determined value of 6.89, it can be concluded that higher pH values Favor biosorption of positively charged Co^{2+} ions. In addition to this value, when choosing the pH value for operating conditions, influence of Co^{2+} ion precipitation in aqueous solutions should be considered as it is pH dependent. Thus, this process was also analysed as shown in Figure 6. At a pH

value of 7.2, only very weak precipitation of $Co(OH)^+$ occurs (0.26 %) while at pH 8.2 somewhat more significant precipitation occurs yielding the distribution of biosorbed cobalt species as 97.1 % Co^{2+}, 2.6 % $Co(OH)^+$, and 0.3 % $Co(OH)_2$. With the intention to avoid the influence of precipitation on biosorption and considering the pH_{PZC} value (6.89) above which biosorption of Co^{2+} is favoured, a pH value of 7 was chosen for conduction of biosorption experiments.

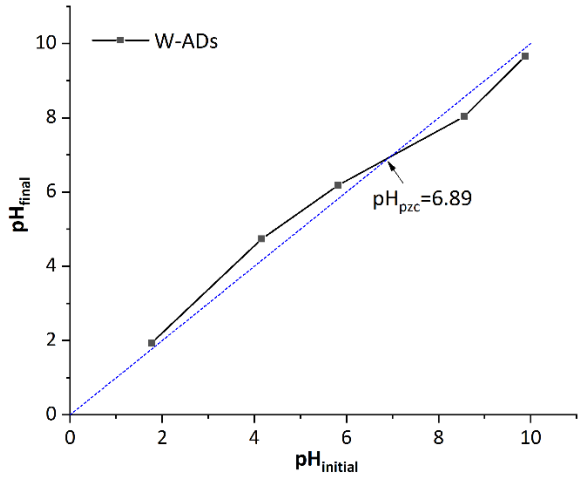

Figure 5. Determination of pH_{pzc} of the W-ADs biosorbent

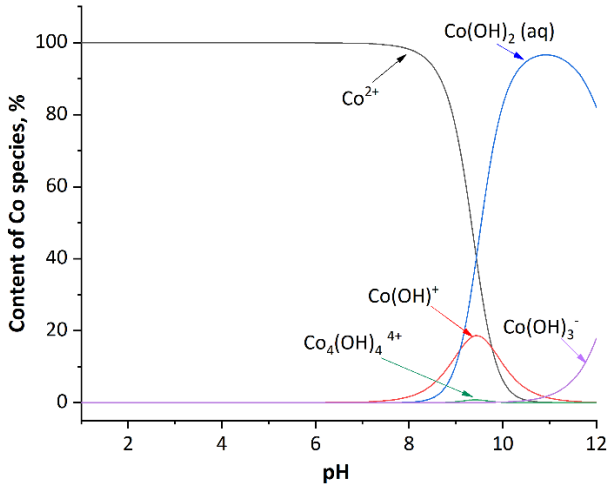

Figure 6. Speciation diagram for Co^{2+} aqueous solution as a function of pH

3. 7. Biosorption kinetics

The kinetics of Co^{2+} biosorption onto the W-ADs biosorbent over time is presented in Figure 7. The biosorbed Co^{2+} amount increased until reaching a maximum value, as expected. The obtained results indicate that the equilibrium was achieved within 360 min. This occurrence is a result of Co^{2+} ions binding to active sites on the biosorbent surfaceAfter about 360 min, saturation of W-ADs functional groups has occurred, and apparent equilibrium was reached.

The experimental results were modelled by using four different models (pseudo-first, pseudo-second, Elovich, and intra-particle diffusion model). For preliminary assessment, the experimental data were fitted by the models in linear forms (Fig. 8). The coefficients of determination *(R^2)* for the best fits of pseudo-first order model, pseudo-second order model, Elovich and intra-particle model were 0.977, 0.964, 0.901 and 0.930, respectively, showing apparently good agreements with the experimental data except for the Elovich model, which clearly deviated from the experimental data. Weaknesses of linear correlations can be observed when the experimental data were fitted with models in non-linear forms. Certain values of the coefficient of determination for a model in linear and non-linear form can quantitatively show the difference [13].

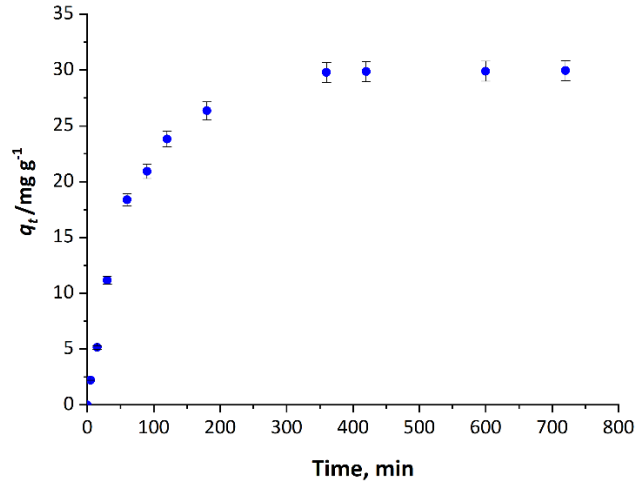

Figure 7. Biosorbed amount of Co^{2+} per the W-ADs biosorbent content over time

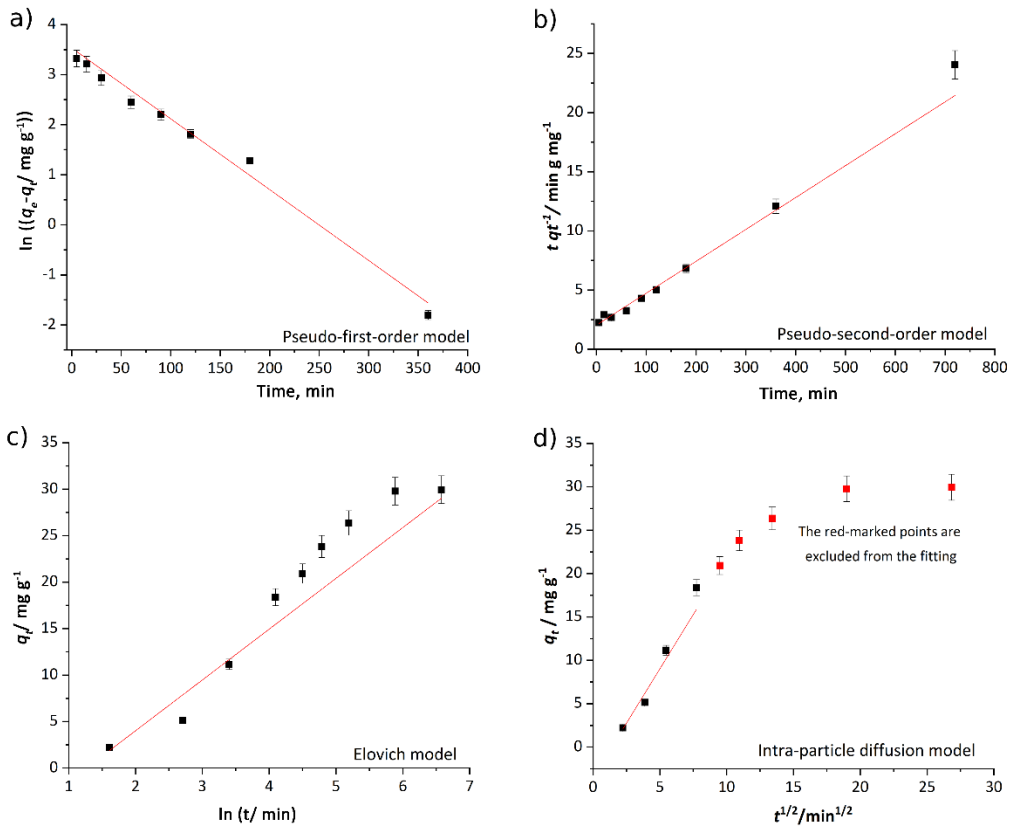

Figure 8. Kinetic plots for linear modelling of experimental biosorption data (symbols) for: a) pseudo- first order model, b) pseudo-second order model, c) Elovich model, and d) intra-particle diffusion model applied for the initial biosorption period up to $q_t/q_e < 0.4$

Considering this fact and the close values of the coefficient of determination obtained by applying the pseudo-second order, pseudo-first order, and the intra-particle diffusion model, these models were applied in non-linear forms as more precise. The results of modelling in non-linear forms are shown in Table 2. It can be seen that the linear and non-linear regression methods yielded different values of model parameters (Fig. 8 and Table 2). The coefficients of determination obtained by applying non-linear forms of the pseudo-first and pseudo-second order model were higher, while that of the intra-particle diffusion model was lower, which clearly shows how using only the linear form of a model can lead to erroneous conclusions. In order to determine the best model for biosorption kinetics it is recommended to observe the value of chi-square (χ^2) obtained by the non-linear regression method along with R^2 values [27,28] presented also in Table 2. The obtained kinetic parameters for the pseudo-first order, pseudo-second order, and the intra-particle diffusion models revealed that the pseudo-first order kinetic model provided the best agreement with experimental data, with the highest coefficient of determination and a lowest chi-square value. Additionally, this can be seen by comparison of the model predictions with the experimental data indicating the pseudo-first order model as the best (Fig. 9).

Table 2. Kinetic parameters obtained by non-linear regression analyses of different kinetic models applied to the experimental data for biosorption of Co^{2+} ions onto W-ADs biosorbent

Pseudo-first order model			
q_e / mg g^{-1}	k_1 / min^{-1}	R^2	χ^2
29.48	1.46×10^{-2}	0.996	0.757
Pseudo-second order model			
q_e / mg g^{-1}	k_2 / g mg^{-1} min^{-1}	R^2	χ^2
33.83	5.24×10^{-4}	0.991	0.851
Intra-particle diffusion model			
	K_{dif} / mg g^{-1} min$^{-0.5}$	R^2	χ^2
	1.52	0.741	15.86

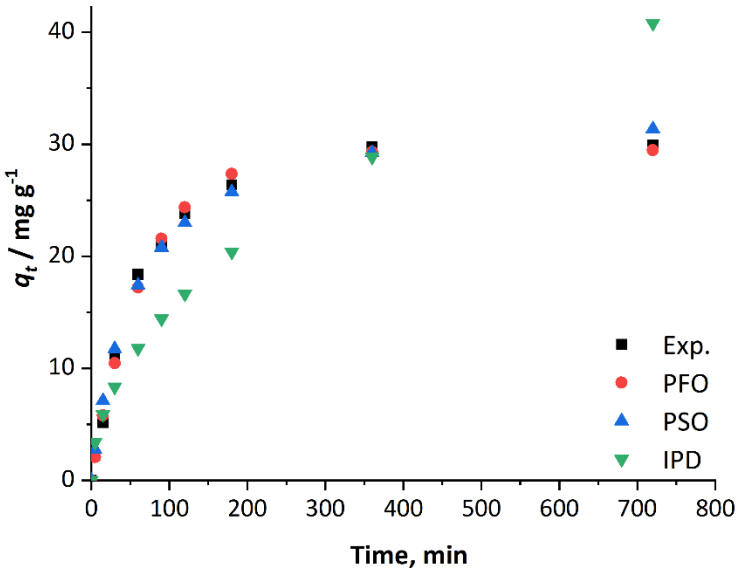

Figure 9. Biosorption experimental data and best model predictions obtained by non-linear fitting for the pseudo-first order (PFO), pseudo-second order (PSO), and intra-particle diffusion model (IPD)

Comparative kinetic data and equilibrium biosorbent capacities assessment for Co^{2+} ions removal using *Arundo donax* and various biomass biosorbents is given in Table 3.

Table 3. Comparison of kinetic modeling results (pseudo-first order (PFO) and pseudo-second order (PSO), and equilibrium biosorbent capacities of Co^{2+} ions removal using different types of biosorbents

Biosorbent	Kinetic model	R^2	Rate constant		q_e/ mg g^{-1}	Ref.
Aspergillus flavus biomass	PSO	0.999	k_2 / g mg^{-1} min^{-1}	0.0270	12.47	[29]
Pre-treated *2-Hypnea Valentiae* algae biomass	PSO	0.980	k_2 / g mg^{-1} min^{-1}	0.0072	10.98	[30]
Cocos nucifera L. leaf powder	PSO	0.997	k_2 / g mg^{-1} min^{-1}	0.1238	1.430	[31]
Modified corn silk	PSO	0.997	k_2 / g mg^{-1} min^{-1}	0.0867	9.164	[32]
Saccharum bengalense (SB)	PSO	0.903	k_2 / g mg^{-1} min^{-1}	0.0184	4.62	[33]
Alginate extracted from marine red algae biomass (*Callithamnion corymbosum* sp.)	PSO	0.999	k_2 / g mg^{-1} min^{-1}	0.0291	13.64	[34]
Lignocellulosic biosorbent-coir pith	PSO	0.990	k_2 / g mg^{-1} min^{-1}	0.0200	8.540	[35]
Spent coffee (SC)	PSO	0.999	k_2 / g mg^{-1} min^{-1}	0.1340	3.741	[36]
Arundo donax stems W-ADs biosorbent	PFO	0.977	k_1 / min^{-1}	0.0141	29.48	This study

According to the data in Table 3, the pseudo-first order and pseudo-second order kinetic models were used for describing the biosorption kinetics of Co^{2+} ions by biosorbents derived from different biomass sources, the pseudo-second order being the best in all cases, except for this study. By comparing the equilibrium capacities for Co ions for different biosorbents it was shown that biosorbent used in this study (W-Ads) is better than others.

4. CONCLUSION

Biosorbents derived from plant biomass can be promising materials for the removal of metal ions from aqueous solutions. This work investigated the possibility of using *Arundo donax* stems (W-Ads) as a natural, and inexpensive biosorbent to eliminate Co^{2+} ions from an aqueous solution. The biosorbent was characterized by using chemical composition analysis, the point of zero charge (pH_{PZC}) determination, SEM, EDS, XRD, and FTIR analyses. The conducted kinetic studies demonstrate the biosorbed amount of Co^{2+} increased with time until reaching a maximum value after approximately 360 min. In this research, the experimental kinetic data were analyzed using four different kinetic models (pseudo-first, pseudo-second, Elovich, and intra-particle diffusion model). The pseudo-first kinetic model provided the best agreement with experimental data confirmed with the highest coefficient of determination $R^2 = 0.996$, and a lowest $\chi^2 = 0.757$. The results obtained in this study can be used for scale-up in the design of batch biosorption systems for cobalt removal from aqueous solutions.

Acknowledgments: This work was financially supported by the Ministry of Science, Technological Development and Innovation of the Republic of Serbia (Grant No 451-03-47/2023-14/200026).

REFERENCES

[1] Graedel TE, Gunn G, Tercero Espinoza L. Metal resources, use and criticality. *Critical Metals Handbook.* 1st ed., Chichester, UK: John Wiley & Sons; 2014: 1-19. https://doi.org/10.1002/9781118755341.ch1.

[2] Awual MR, Hasan MM, Islam A, Asiri AM, Rahman MM. Optimization of an innovative composited material for effective monitoring and removal of cobalt(II) from wastewater. *J Mol Liq.* 2020; 298: 112035. https://doi.org/10.1016/j.molliq.2019.112035.

[3] Agarwal A, Upadhyay U, Sreedhar I, Singh SA, Patel CM. A review on valorization of biomass in heavy metal removal from wastewater. *J Water Process Eng.* 2020; 38: 101602. https://doi.org/10.1016/j.jwpe.2020.101602.

[4] Aryal M. A comprehensive study on the bacterial biosorption of heavy metals: Materials, performances, mechanisms, and mathematical modellings. *Rev Chem Eng.* 2021; 37 (6): 715-754. https://doi.org/10.1515/revce-2019-0016.

[5] Guleria A, Kumari G, Lima EC, Ashish DK, Thakur V, Singh K. Removal of inorganic toxic contaminants from wastewater using sustainable biomass: A review. *Sci Total Environ.* 2022; 823: 153689. https://doi.org/10.1016/j.scitotenv.2022.153689.

[6] Zhang D, Jiang QW, Liang DY, Huang S, Liao J. The Potential Application of Giant Reed (Arundo donax) in Ecological Remediation. *Front Environ Sci.* 2021; 9: 652367. https://doi.org/10.3389/fenvs.2021.652367.

[7] Deng H, Ye ZH, Wong MH. Accumulation of lead, zinc, copper and cadmium by 12 wetland plant species thriving in metal-contaminated sites in China. *Environ Pollut.* 2004; 132 (1): 29–40. https://doi.org/10.1016/j.envpol.2004.03.030.

[8] Nsanganwimana F, Marchand L, Douay F, Mench M. Arundo donax L., a Candidate for Phytomanaging Water and Soils Contaminated by Trace Elements and Producing Plant-Based Feedstock. A Review. *Int J Phytoremediation.* 2014; 16 (10): 982–1017. https://doi.org/10.1080/15226514.2013.810580.

[9] Mavrogianopoulos G, Vogli V, Kyritsis S. Use of wastewater as a nutrient solution in a closed gravel hydroponic culture of giant reed (Arundo donax). *Bioresour Technol.* 2002; 82 (2): 103–107. https://doi.org/10.1016/S0960-8524(01)00180-8.

[10] Song HL, Liang L, Yang KY. Removal of several metal ions from aqueous solution using powdered stem of Arundo donax L: As a new biosorbent. *Chem Eng Res Des.* 2014; 92 (10): 1915–1922. https://doi.org/10.1016/j.cherd.2014.04.027.

[11] ISO 16472:2006: Animal feeding stuffs — Determination of amylase-treated neutral detergent fibre content (aNDF), 2006.

[12] ISO 13906:2008: Animal feeding stuffs — Determination of acid detergent fibre (ADF) and acid detergent lignin (ADL) contents 2008.

[13] Abatal M, Anastopoulos I, Giannakoudakis DA, Olguin MT. Carbonaceous material obtained from bark biomass as adsorbent of phenolic compounds from aqueous solutions. *J Environ Chem Eng.* 2020; 8 (3): 103784. https://doi.org/10.1016/j.jece.2020.103784.

[14] Wang J, Guo X. Adsorption kinetic models: Physical meanings, applications, and solving methods. *J Hazard Mater.* 2020; 390: 122156. https://doi.org/10.1016/j.jhazmat.2020.122156.

[15] Obradovic B. Guidelines for general adsorption kinetics modeling. *Hem Ind.* 2020; 74 (1): 65–70. https://doi.org/10.2298/HEMIND200201006O.

[16] Bessa W, Trache D, Derradji M, *et al.* Characterization of raw and treated Arundo donax L. cellulosic fibers and their effect on the curing kinetics of bisphenol A-based benzoxazine. *Int J Biol Macromol.* 2020; 164: 2931–2943. https://doi.org/10.1016/j.ijbiomac.2020.08.179.

[17] You T, Wang R, Zhang X, Ramaswamy S, Xu F. Reconstruction of lignin and hemicelluloses by aqueous ethanol anti-solvents to improve the ionic liquid-acid pretreatment performance of Arundo donax Linn. *Biotechnol Bioeng.* 2018; 115 (1): 82–91. https://doi.org/10.1002/bit.26457.

[18] Suárez L, Barczewski M, Kosmela P, Marrero MD, Ortega Z. Giant Reed (Arundo donax L.) Fiber Extraction and Characterization for Its Use in Polymer Composites. *J Nat Fibers.* 2023; 20 (1): 1–15. https://doi.org/10.1080/15440478.2022.2131687.

[19] Krička T, Matin A, Bilandžija N, *et al.* Biomass valorisation of Arundo donax L., Miscanthus × giganteus and Sida hermaphrodita for biofuel production. *Int Agrophysics.* 2017; 31 (4): 575–581. https://doi.org/10.1515/intag-2016-0085.

[20] Barana D, Salanti A, Orlandi M, Ali DS, Zoia L. Biorefinery process for the simultaneous recovery of lignin, hemicelluloses, cellulose nanocrystals and silica from rice husk and Arundo donax. *Ind Crops Prod.* 2016; 86: 31–39. https://doi.org/10.1016/j.indcrop.2016.03.029.

[21] Shatalov AA, Pereira H. Papermaking fibers from giant reed (Arundo donax L.) by advanced ecologically friendly pulping and bleaching technologies. *BioResources.* 2006; 1 (1): 45–61. https://doi.org/10.15376/biores.1.1.45-61.

[22] Zhuang J, Li M, Pu Y, Ragauskas AJ, Yoo CG. Observation of potential contaminants in processed biomass using fourier transform infrared spectroscopy. *Appl Sci.* 2020; 10 (12): 1–13. https://doi.org/10.3390/app10124345.

[23] Fiore V, Scalici T, Valenza A. Characterization of a new natural fiber from Arundo donax L. as potential reinforcement of polymer composites. *Carbohydr Polym.* 2014; 106 (1): 77–83. https://doi.org/10.1016/j.carbpol.2014.02.016.

[24] Galia A, Schiavo B, Antonetti C, *et al.* Autohydrolysis pretreatment of Arundo donax: A comparison between microwave-assisted batch and fast heating rate flow-through reaction systems. *Biotechnol Biofuels.* 2015; 8 (1): 1–18.

https://doi.org/10.1186/s13068-015-0398-5.

[25] Raspolli Galletti AM, D'Alessio A, Licursi D, *et al.* Midinfrared FT-IR as a tool for monitoring herbaceous biomass composition and its conversion to furfural. *J Spectrosc.* 2015; 2015 (1): 1-12. https://doi.org/10.1155/2015/719042.

[26] Payá J, Roselló J, Monzó JM, *et al.* An approach to a new supplementary cementing material: Arundo donax straw ash. *Sustain.* 2018; 10 (11): 4273. https://doi.org/10.3390/su10114273.

[27] Obradovic B. Back to basics: Avoiding errors in scientific research and publications. *Hem Ind.* 2019; 73 (3):143–146. https://doi.org/10.2298/HEMIND190630018O.

[28] Ezeonuegbu BA, Machido DA, Whong CMZ, *et al.* Agricultural waste of sugarcane bagasse as efficient adsorbent for lead and nickel removal from untreated wastewater: Biosorption, equilibrium isotherms, kinetics and desorption studies. *Biotechnol Reports.* 2021; 30: e00614. https://doi.org/10.1016/j.btre.2021.e00614.

[29] Foroutan R, Esmaeili H, Rishehri SD, *et al.* Zinc, nickel, and cobalt ions removal from aqueous solution and plating plant wastewater by modified Aspergillus flavus biomass: A dataset. *Data Br.* 2017; 12: 485–492. https://doi.org/10.1016/j.dib.2017.04.031.

[30] Vafajoo L, Cheraghi R, Dabbagh R, McKay G. Removal of cobalt (II) ions from aqueous solutions utilizing the pre-treated 2-Hypnea Valentiae algae: Equilibrium, thermodynamic, and dynamic studies. *Chem Eng J.* 2018; 331 : 39–47. https://doi.org/10.1016/j.cej.2017.08.019.

[31] Hymavathi D, Prabhakar G. Optimization, equilibrium, and kinetic studies of adsorptive removal of cobalt(II) from aqueous solutions using Cocos nucifera L. *Chem Eng Commun.* 2017; 204 (9): 1094–1104. https://doi.org/10.1080/00986445.2017.1338570.

[32] Yu H, Pang J, Ai T, Liu L. Biosorption of Cu2+, Co2+ and Ni2+ from aqueous solution by modified corn silk: Equilibrium, kinetics, and thermodynamic studies. *J Taiwan Inst Chem Eng.* 2016; 62: 21–30. https://doi.org/10.1016/j.jtice.2016.01.026.

[33] Imran Din M, Mirza ML, Ata S, Athar M, Mohsin IU. Thermodynamics of biosorption for removal of Co(II) ions by an efficient and ecofriendly biosorbent (saccharum bengalense): Kinetics and isotherm modeling. *J Chem.* 2013; 2013: 1-11. https://doi.org/10.1155/2013/528542.

[34] A. R. Lucaci, D. Bulgariu, I. Ahmad. Equilibrium and Kinetics Studies of Metal Ions Biosorption on Alginate Extracted from Marine Red Algae Biomass (Callithamnion corymbosum sp.). *J Polym.* 2020; 12 (9): 1–16. https://doi.org/10.3390/polym12091888

[35] Parab H, Joshi S, Sudersanan M, Shenoy N, Lali A, Sarma U. Removal and recovery of cobalt from aqueous solutions by adsorption using low cost lignocellulosic biomass-coir pith. *J Environ Sci Heal - Part A Toxic/Hazardous Subst Environ Eng.* 2010; 45 (5): 603–611. https://doi.org/10.1080/10934521003595662.

[36] Imessaoudene D, Hanini S, Bouzidi A, Ararem A. Kinetic and thermodynamic study of cobalt adsorption by spent coffee. *Desalin Water Treat.* 2016; 57 (13): 6116–6123. https://doi.org/10.1080/19443994.2015.1041049.

Valorizacija energetske biljke *Arundo donax* uzgajane u Srbiji za biosorpciju jona kobalta iz vodenog rastvora: kinetički aspekt

Jovana Perendija[1], Dragana Milošević[1], Mina Popović[1], Željko Dželetović[2], Sabina Kovač[3], Jasmina Grbović Novaković[4] i Slobodan Cvetković[1]

[1]Univerzitet u Beogradu-Institut za hemiju, tehnologiju I metalurgiju, Institut od nacionalnog značaja za RepublikuSrbiju, Beograd, Srbija
[2]Univerzitet u Beogradu, Institut za primenu nuklearne energije- INEP, Zemun- Beograd, Srbija
[3]Univerzitet u Beogradu, Rudarsko-geološki fakultet, Beograd, Srbija
[4]Univerzitet u Beogradu, Institut za nuklearne nauke "Vinča", Institut od nacionalnog značaja za Republiku Srbiju, Centar izvrsnosti: "Centar za vodoničnu energiju i obnovljive izvore energije", Beograd, Srbija

(Naučni rad)

Izvod

Joni metala se mogu eliminisati iz vodenih rastvora korišćenjem biosorbenata, materijala dobijenih iz biljne biomase. U ovoj studiji, istraživana je potencijalna upotreba *Arundo donax* stabljike kao jeftinog, prirodnog biosorbenta za uklanjanje jona kobalta (Co^{2+}) iz vodenog rastvora. *Arundo donax* stabljika je karakterisana analizom hemijskog sastava (u pogledu sadržaja celuloze, hemiceluloze i lignina), tačke nultog naelektrisanja (pH_{PZC}), skenirajućom elektronskom mikroskopijom (*SEM*), energetskom disperzionom spektroskopijom x–zraka (*EDS*), rendgenskom difrakcionom analizom (*XRD*) i infracrvenom spektroskopijom sa Furijeovom transformacijom (*FTIR*). Istraživanja kinetike su pokazala da se vezana količina Co^{2+} jona na *Arundo donax* stabljici povećavala sa povećanjem vremena kontakta dostižući stanje ravnoteže posle 360 min. Primenjeni su kinetički modeli pseudo-prvog reda, pseudo-drugog reda, Eločičev model i model unutrašnje difuzije za opisivanje eksperimentalnih podataka. Najbolja predviđanja su dobijena primenom kinetičkog modela pseudo-prvog reda uz najveću vrednost koeficijenta determinacije R^2 = 0.996, i najmanju vrednost χ^2 = 0.757. Nalazi ove studije mogu se primeniti na projektovanje šaržnih biosorpcionih sistema za uklanjanje jona kobalta iz vodenih rastvora.

Ključne reči: biosorbent; Co^{2+} joni; karakterizacija Arundo Donax; kinetičko modelovanje